Reflection of a Gaussian beam at a nonlinear interface

W. J. Tomlinson, J. P. Gordon, P. W. Smith, and A. E. Kaplan

By numerical simulations of the reflection of a (2-D) Gaussian beam from a nonlinear interface, we show several new features of the behavior of such an interface and resolve the difference between the results of two previous studies of this type. Newly reported features include a very large nonlinear Goos-Hänchen shift and large variations of the angle of an output beam for small changes in the input intensity. The latter phenomenon has potential applications for a light-controlled angular scanning element. The differences between prior studies of this type are shown to be an artifact of the numerical procedures used.

I. Introduction

It has been proposed that the interface between a nonlinear (optical Kerr effect) medium and a linear medium, a nonlinear interface, can serve as a new type of nonlinear optical element.[1] Theoretical studies have suggested that such an interface can exhibit total reflection for input beams with intensities below a critical value and substantially reduced reflectivity for higher intensities. An optical element with such a threshold behavior is potentially useful for optical switching and logic, and because the nonlinear interface does not involve any resonator, with appropriate materials it offers the possibility of ultrafast (subpicosecond) switching. To assess that potential it is necessary to understand the detailed behavior of such interfaces, but this has proven to be a challenging problem, with various investigators reporting conflicting results.[2-5]

We report here on some detailed numerical simulations of the behavior of nonlinear interfaces. Our analysis shows several new features of that behavior and explains the difference between the results of two previous studies. As the intensity of the input beam is increased from zero the first consequence of the nonlinearity is a very large and nonlinear Goos-Hänchen shift not previously reported. At higher intensities the light penetrates into the nonlinear medium and propagates in a narrow self-focused channel. We show here that the propagation direction of this channel is a sensitive function of the light intensity. This phenomenon is potentially useful for producing a light-driven angular scanning element. Our results indicate that an input Gaussian beam in the linear medium cannot couple to an optical surface wave, in disagreement with an earlier study of this type[5] but consistent with a recent theoretical analysis.[6]

For the case in which the input beam is an infinite plane wave Kaplan has derived an analytical theory of nonlinear interfaces,[1] but the assumptions used in deriving that theory, and the interpretation of the results, have been the subject of a controversy that has yet to be resolved. Much of this controversy has concerned the prediction that such an interface can have a bistable reflectivity. The only available experimental results[7,8] are consistent with this prediction but are themselves difficult to interpret and cannot be considered conclusive.

In any experiment, and certainly in any practical device, the input beam will have a finite width, and this leads to a theoretical problem of such complexity that to date it has only been treated by numerical techniques. In fact, thus far it has only been possible to analyze the case of 2-D beams, in which it is assumed that all the optical fields extend uniformly to infinity in the direction normal to the plane of incidence.

Two such studies have been reported, both dealing with the situation in which an input beam in the linear medium is totally internally reflected at the interface for low input intensities and the nonlinear medium has a positive Kerr constant.[4,5] Although the specific parameter values used were different, it is notable that these two studies predicted qualitatively different behavior. The most notable difference is that for input intensities above a threshold value one calculation gave a transmitted beam in the form of a self-focused channel or channels, while the other calculation showed a portion of the light coupled into an optical surface wave,[9,10] with little or no transmitted light.

In the present paper we have used numerical simu-

A. E. Kaplan is with MIT Francis Bitter National Laboratory, Cambridge, Massachusetts 02139; the other authors are with Bell Laboratories, Holmdel, New Jersey 07733.

Received 22 December 1981.
0003-6935/82/112041-11$01.00/0.

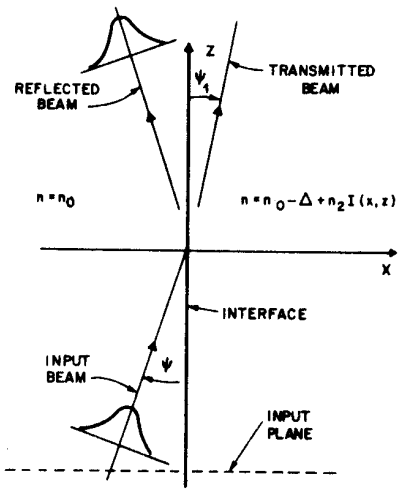

Fig. 1. Interface configuration and coordinate system.

lation to make a detailed study of the behavior of one particular interface and input beam configuration as a function of the intensity of the input beam. Even with the largest computers currently available it is not feasible to fully explore wide ranges of interface and input beam parameters, so we have concentrated on obtaining a very detailed understanding of the behavior of this one particular configuration and on developing physical interpretations of that behavior.

The organization of this paper is as follows. In Sec. II we define the particular configuration we are studying, review the basic phenomena expected at a nonlinear interface, and summarize the results of the plane wave theory. We have organized this material in short subsections so that readers can easily skim over those topics with which they are already familiar. In Sec. III we describe the computational techniques we have used, with some of the more technical details reserved for the Appendix. Section IV contains the results of our calculations, and in Sec. V we present our conclusions.

II. Background

A. Configuration and Coordinate System

The basic interface configuration and coordinate system we consider in this paper is illustrated in Fig. 1. The interface is the y-z plane, with the linear medium having a refractive index n_0 on the left ($x < 0$), and the nonlinear medium on the right ($x > 0$). We assume that the refractive index of the nonlinear medium is of the form

$$n(x,y,z) = n_0 - \Delta + n_2 I_1(x,y,z), \tag{1}$$

where $I_1(x,y,z)$ is the intensity of the light in the nonlinear medium at the point (x,y,z), and Δ and n_2 are small positive constants. With this configuration, a low-intensity beam incident on the interface from the linear medium side at a sufficiently shallow angle will be totally reflected at the interface.

We assume that the input beam is a 2-D Gaussian beam, with its axis at an angle ψ with respect to the interface. We should emphasize that we are treating only a 2-D system, i.e., the fields are assumed to be independent of the y coordinate (normal to the plane of the figure). For all the calculations described in this paper the input beam was defined such that it propagates in the direction of increasing z and its focus is centered on the origin ($x = z = 0$).

As described above, we have chosen to do most of our calculations for a single set of interface and input beam parameters. We have chosen an interface with $n_0 = 1.5$ and $\Delta = 0.02$. This gives a low-intensity critical angle of $\psi_c \equiv (2\Delta/n_0)^{1/2} = 9.4°$. We have chosen an input beam at an angle $\psi = 5°$, with a $1/e$ amplitude radius at its focus of $w_0 = 10\lambda$, where λ is the vacuum wavelength of the light, and for simplicity we have set $\lambda = 1$. Such a beam has a far-field diffraction half-angle of 1.22° (in the linear medium) so that for low intensities it will be totally reflected at the interface.

Our basic goal in this paper is to study the behavior of this interface as a function of the intensity of the input beam. However, this behavior is actually determined by the product of the beam intensity and the Kerr constant n_2 of the nonlinear medium, and we have found it convenient to use a constant input intensity and vary the value of n_2. We defined the input beam to have a peak intensity of unity at its focus ($x = z = 0$).

B. Reflection of a Gaussian Beam at a Linear Interface

As an aid in interpreting our results for nonlinear interfaces and to introduce the format we will use to present our results, in this section we briefly review the behavior of a linear interface for an incident Gaussian beam. The linear interface is a much simpler (but nontrivial) problem because one can make use of linear superposition to express the input beam as an expansion in terms of plane wave components, apply the Fresnel equations to calculate the reflection and transmission of each component, and then add up all the resulting plane wave components to get the reflected and transmitted beams. (See, for example, Ref. 11 and references therein.)

Using linear superposition we have calculated the intensity distributions for several z = constant planes for our assumed interface and input beam parameters (but with $n_2 = 0$). In Fig. 2(a) (for $z = -200$) we see the input Gaussian beam profile. Note that the beam is focused at $z = 0$. At $z = -200$ it has a radius of $w = 10.9$ and a peak intensity of slightly <1.0. Also note that this plot is for a plane of constant z, while the beam propagation direction is tilted 5° with respect to the normal to this plane. We have only plotted the intensity distribution, but a similar plot of the phase of the field would show a curved phase front converging toward the focus.

In Fig. 2(b) we show the intensity distribution on the plane $z = 0$. On this plane the incident and reflected fields are almost equal, and they interfere to give

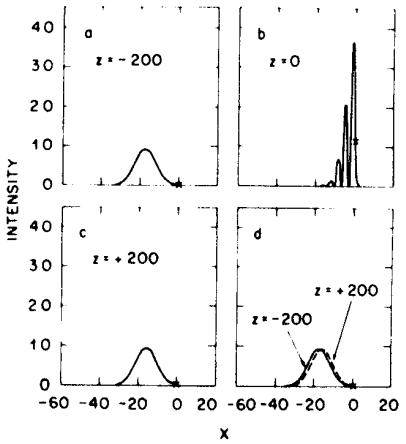

Fig. 2. Intensity distributions on various constant-z planes for a linear interface ($n_2 = 0$): (a) $z = -200$; (b) $z = 0$; (c) $z = +200$; (d) comparison of distributions at $z = -200$ and $+200$.

high-contrast fringes with a period $\Lambda = \lambda/(2n \sin\psi) = 3.82$. The × on the curve indicates the intensity at the interface. Note that, because of the constructive interference between the incident and reflected beams, the intensity at the interface is 1.13 as compared with a peak intensity of unity for the input beam.

The intensity distribution on the plane $z = +200$ shown in Fig. 2(c) is again a Gaussian beam, indicating that the beam has been totally reflected. However, a more careful comparison of the distributions at $z = -200$ and $+200$ [see Fig. 2(d)] shows that they are not identical. This phenomenon is the Goos-Hänchen shift and is a result of the fact that while the various plane wave components of the input beam are all totally reflected, they experience different phase shifts and thus do not add up to give an exact (geometric) reflection of the input beam. The major effect of this is an apparent translation of the reflected beam parallel to the geometric reflection of the input beam (in this case by ~3.4) and a translation of the apparent focus along the beam axis (in this case by ~15.4). There are other higher-order differences, but in the linear case they are generally negligibly small. An alternate physical picture of the Goos-Hänchen shift is that it is a result of some of the power in the input beam flowing along the interface (in the lower-index medium), thus shifting the reflected beam along the interface. We will see that this is a convenient picture to use when considering the behavior of the nonlinear interface.

The format we have chosen to present many of our results is a 3-D perspective plot showing the intensity distributions on a set of planes of constant z. In Fig. 3 we show such a plot for the linear interface. (The curves for $z = -200$, 0, and $+200$ are the same data as are plotted in Fig. 2.) In addition to the intensity distributions the plot also includes a broken line joining the points where the various distributions intersect the interface. This line helps to emphasize the location of the interface and indicates the general behavior of the intensity along the interface.

C. Basic Phenomena at a Nonlinear Interface

Starting from the behavior of the linear interface just described we can use simple physical arguments to estimate the types of behavior that might occur at a nonlinear interface. As the nonlinear coefficient is increased from zero (or alternately, as the intensity is increased with a fixed nonlinearity) the evanescent field in the nonlinear medium will act through the nonlinearity to reduce the refractive-index difference at the interface, thus reducing the effective critical angle. Moving the effective critical angle closer to the incident angle generally results in an increase in the evanescent field. This produces a positive feedback effect in which an increase of the input intensity increases the evanescent field, which reduces the effective critical angle, which further increases the evanescent field. On the basis of this simple physical picture it seems reasonable to expect that there will be some threshold input intensity at which there will be a sudden switch from total internal reflection (TIR) to a state with both transmitted and reflected beams.

We can estimate the threshold intensity from the linear interface results given above. To have a critical angle equal to the angle of our input beam (5°) a linear interface would need an index difference $\Delta = 0.0057$. From Eq. (1) a nonlinear interface with $\Delta = 0.02$ would have this index difference if $n_2 I_1(x = 0) = 0.0143$. From Fig. 2(b) we see that for a linear interface with $\Delta = 0.02$ our input beam with a peak intensity of unity gives a peak intensity of 1.13 at the interface. Therefore we estimate that the threshold for this beam at a nonlinear interface will be at $n_2 \sim 0.0143/1.13 = 0.0126$, with the positive feedback effect described above probably resulting in a somewhat lower threshold. (The actual value determined from our numerical calculations is $n_2 = 0.0112$.)

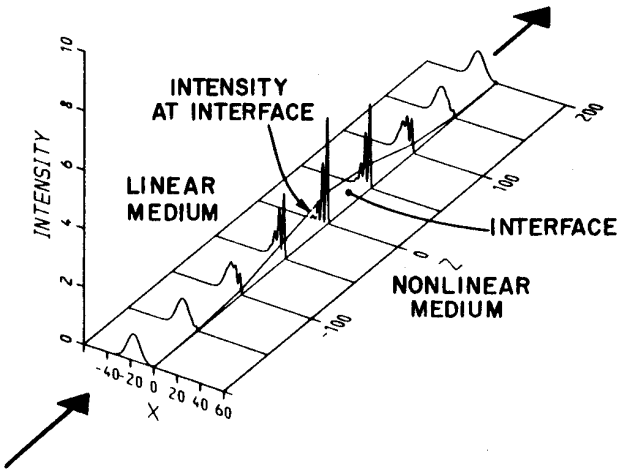

Fig. 3. Perspective plot showing intensity distributions for a linear interface ($n_2 = 0$). This format is used to present many of the results for nonlinear interfaces.

D. Plane Wave Theory

The plane wave theory of a nonlinear interface[1] is a useful reference point for the analysis of the Gaussian beam case. The plane wave theory is also relevant in our present study because our results provide some information that can be used to analyze various criticisms of the plane wave theory. Therefore, in this section we briefly summarize the predictions of the plane wave theory and the criticisms of the theory.

The plane wave theory is based on three simple assumptions: (1) the input field is an infinite plane wave; (2) the reflected field is an infinite plane wave; (3) the field in the nonlinear medium is either a transmitted infinite plane wave, or an evanescent field which decreases monotonically with distance from the interface x but is independent of the y or z coordinates. With these assumptions Kaplan was able to find a set of closed-form analytical solutions of the scalar wave equation that satisfies all the relevant boundary conditions.[1,12] These solutions have been obtained both for positive nonlinearities[1] and for negative nonlinearities,[1,12] but in the present work we only consider positive nonlinearities.

The theory predicts that there will be a sudden jump from TIR to partial transmission at a threshold input intensity I_0 given by

$$\frac{n_2 I_0}{\Delta} = \begin{cases} \frac{1}{2}[1 - (\psi/\psi_c)^2] & 1/\sqrt{2} \le \psi/\psi_c < 1 \\ \frac{1}{8}(\psi_c/\psi)^2 & 0 < \psi/\psi_c \le 1/\sqrt{2}. \end{cases} \tag{2}$$

For our assumed interface and beam parameters this predicts a threshold of $n_2 I_0 = 0.0088$.

For intensities above a value I_{TIR}, defined by $n_2 I_{\mathrm{TIR}}/\Delta = \frac{1}{4}[1 - (\psi/\psi_c)^2]$, the theory predicts that there is a transmitted wave solution, with the (amplitude) reflectivity of the interface r and the angle of the transmitted plane wave ψ_1 related to the input intensity I by

$$\frac{n_2 I}{\Delta} = \frac{1}{(1+r)^2}\left[1 - \frac{4r}{(1+r)^2}\left(\frac{\psi}{\psi_c}\right)^2\right], \tag{3}$$

$$\frac{n_2 I}{\Delta} = \frac{(\psi + \psi_1)^2(\psi_1^2 + \psi_c^2 - \psi^2)}{4\psi^2\psi_c^2}. \tag{4}$$

Complete theoretical expressions for the fields can be found in Ref. 1, but for later reference we note that for the TIR solution the amplitude of the field in the nonlinear medium is of the form

$$E(x) = E_0 \operatorname{sech}(k_x x - x_0), \tag{5}$$

where

$$k_x = \frac{2\pi}{\lambda}\sqrt{2n_0\Delta}\,\sqrt{1 - (\psi/\psi_c)^2}, \tag{6}$$

and x_0 is negative.

In Fig. 4 we have plotted the plane wave reflectivity as a function of intensity for the case $\psi/\psi_c = 1/\sqrt{2}$. The most notable feature of this result is that there is a finite range of intensities for which both TIR and transmitted wave solutions exist, so the reflectivity is predicted to be bistable.

Most of the criticisms of the plane wave theory have focused on the assumption that the transmitted field

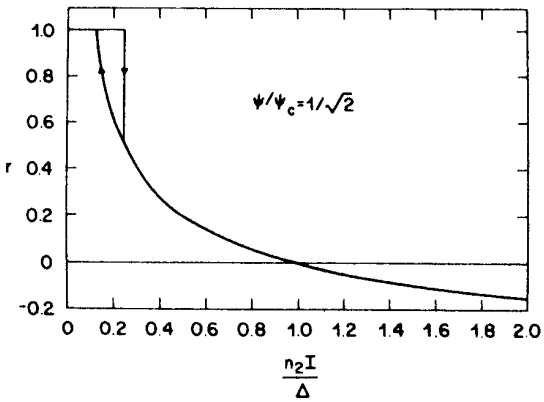

Fig. 4. Plane-wave theory predictions of the amplitude reflectivity of a nonlinear interface for $\psi/\psi_c = 1/\sqrt{2}$ as a function of normalized input intensity.

is a plane wave because it is well-known that a plane wave is not a stable solution in a nonlinear medium with a positive Kerr constant. In such a medium a plane wave will eventually break up into self-focused channels. The key word here is eventually, and it has been suggested that the breakup will take place sufficiently far from the interface that the behavior near the interface will be very close to that predicted by the plane wave theory. No analytical theory has been proposed that can resolve this question. With the precise form of the transmitted wave solution in doubt, the existence of a bistable region for an incident plane wave must be considered uncertain.

E. Surface Wave Theory

The coupling between an incident Gaussian beam and an optical surface wave that was found in a previous numerical study[5] prompted a theoretical study[9] of the characteristics of such a wave. Actually, an almost identical theory[10] had been published by Miyagi and Nishida in 1973. (The surface wave is a form of self-focused channel, except that it is bound to the interface.) In the nonlinear medium the field distribution of the surface wave is of the same form as Eq. (5), except that x_0 is a positive quantity, and k_x is given by

$$k_x = \frac{2\pi}{\lambda}\sqrt{2n_0\Delta}\,\sqrt{1 + D}, \tag{7}$$

where D is a free parameter > 0. A particularly interesting feature of the surface wave is the fact that, independent of the value of the parameter D, the intensity at the interface is always $I_s = 2\Delta/n_2$.

III. Calculational Techniques

The basic equation we are solving is the scalar wave equation

$$\nabla^2 E + n^2 k^2 E = 0, \tag{8}$$

where $k = 2\pi/\lambda$, and E is the complex field amplitude. We define an input-field distribution on a plane of constant z, chosen to be sufficiently far from the in-

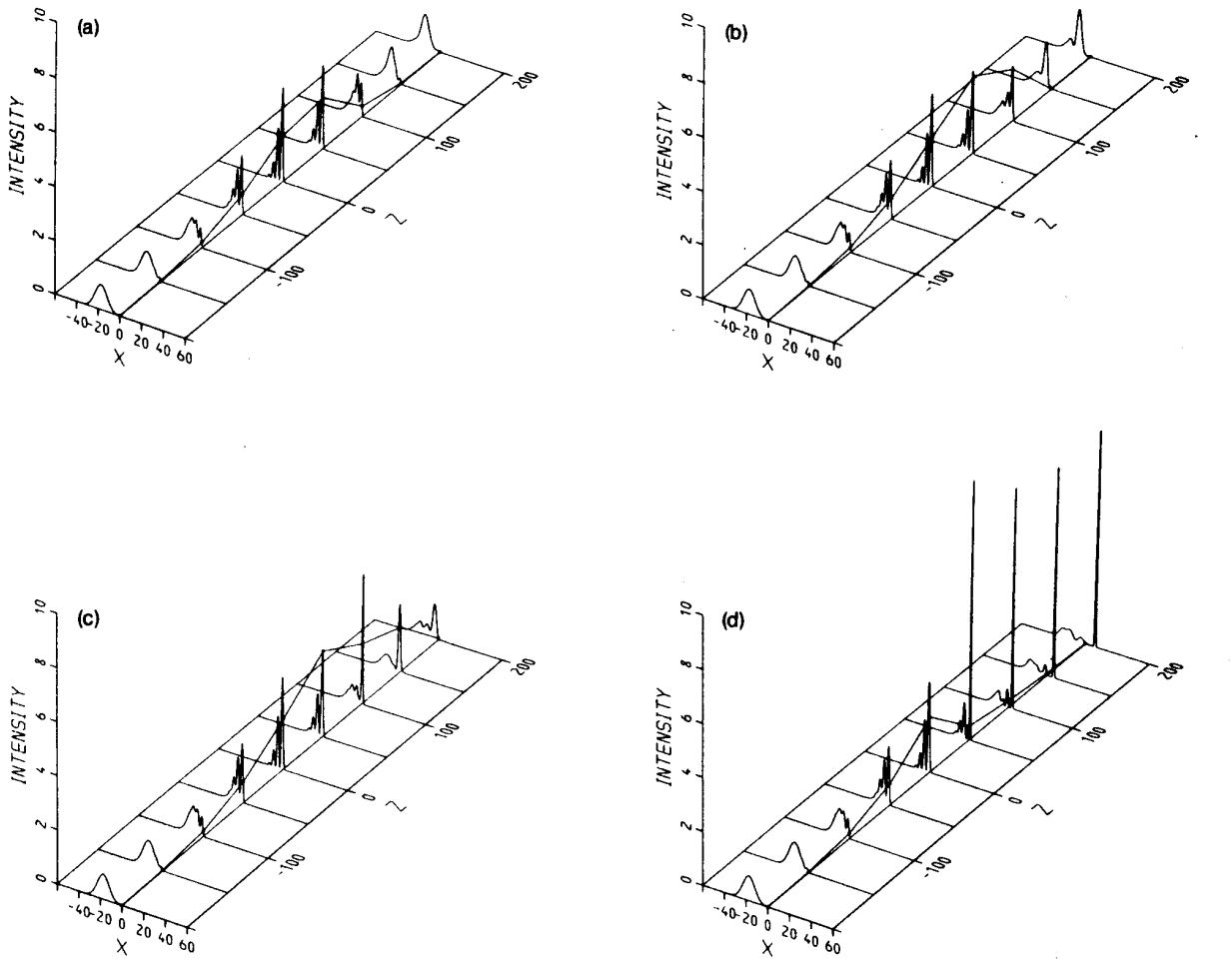

Fig. 5. Perspective plots of the intensity distributions for a nonlinear interface: (a) $n_2 = 0.01000$; (b) $n_2 = 0.01085$; (c) $n_2 = 0.01100$; (d) $n_2 = 0.01200$.

tersection point that on that plane the intensity in the nonlinear medium is negligibly small, and then solve Eq. (8) numerically to determine the field in the rest of the region of interest. For computational efficiency we make a conventional change of variables to a new field variable ϕ defined by

$$E(x,z) = \phi(x,z)\exp(-in_0 k\cos\psi z), \tag{9}$$

in which the exponential factor is an approximation of the most rapidly varying part of the z dependence of the field. With this change of variables Eq. (8) becomes

$$i(2n_0 k\cos\psi)\frac{\partial\phi}{\partial z} = \frac{\partial^2\phi}{\partial z^2} + \frac{\partial^2\phi}{\partial x^2} + (n^2 - n_0^2\cos^2\psi)k^2\phi. \tag{10}$$

We assume that ϕ varies sufficiently slowly with z that we can neglect its second derivative in the z direction [the first term on the right-hand side of Eq. (10)]. This same assumption has been made in all the previous studies of this type.

Equation (10) is solved by treating it as a system of coupled ordinary differential equations, with a pair of equations (for the real and imaginary parts of ϕ) for each point on a uniformly spaced mesh in the x coordinate. The coupling between equations for different x values results from the $\partial^2\phi/\partial x^2$ term. The simplest approximation to this derivative is the three-point formula:

$$\left.\frac{\partial^2\phi}{\partial x^2}\right|_i = \frac{\phi_{i-1} - 2\phi_i + \phi_{i+1}}{\Delta x^2}, \tag{11}$$

but where possible we have used the five-point formula

$$\left.\frac{\partial^2\phi}{\partial x^2}\right|_i = \frac{-\phi_{i-2} + 16\phi_{i-1} - 30\phi_i + 16\phi_{i+1} - \phi_{i+2}}{12\Delta x^2}, \tag{12}$$

where the index i numbers the points in the mesh, and Δx is the point spacing. These formulas cannot be used unless all three (or five) points are on the same side of the interface, because there is a discontinuity in the second (and higher) derivative at the interface. For the point on the interface we used a three-point formula, with a correction term to account for the discontinuity. The derivation of the correction term is given in the Appendix, along with the approximations used for the first and last points.

To solve the system of differential equations we used

the ODES package (ordinary differential equation solver), which is a part of the PORT library of mathematical subroutines.[13] ODES was written by N. L. Schryer and is based on Gragg's modified midpoint rule. The algorithm used is a variable-order variable step-size extrapolation scheme which is locally optimal. That is, at each step in the integration procedure the order and step size are chosen to minimize the cost/unit step in the z coordinate. The calculations were run on a Cray-1 computer, and the program was written to take advantage of the machine's vector processing hardware.

We defined the input distribution on the plane $z = -200$, and used the method of Ref. 11 to calculate the field, assuming $n_2 = 0$. [The input distribution is plotted in Fig. 2(a).] On this plane the intensity at the interface is only 3.3×10^{-3}, so the neglect of the nonlinearity should introduce a negligible error. We set the x boundaries of the calculation at $x = -60$ and $+60$. We investigated the use of various mesh sizes ranging from $\Delta x = 0.6$ (201 points) to $\Delta x = 0.15$ (801 points). It is important to use the coarsest mesh that gives accurate results because the required step size in the z direction varies approximately as Δx^2. For a calculation from $z = -200$ to $z = +200$ with Δx values of 0.6, 0.3, and 0.15, typical processor times were 10, 50, and 350 sec, respectively. (350 sec corresponds to 2.8×10^{10} machine cycles on the Cray-1.)

IV. Results

A. Overview

All the basic features of our results are illustrated in Fig. 5. For the lowest value of the nonlinearity [Fig. 5(a), $n_2 = 0.01$] the behavior of the interface is very similar to that for the linear interface (Fig. 3), but with two differences: (1) the peak intensity at the interface is about twice as high in the nonlinear case and occurs further along the interface; and (2) while the reflected beam is still approximately Gaussian, it is significantly narrower. Both these differences can be described as resulting from an enhanced Goos-Hänchen shift, in which a larger portion of the beam power penetrates into the lower-index medium, and the apparent focus of the reflected beam has been shifted further along its axis.

For a slightly higher nonlinearity [Fig. 5(b), $n_2 = 0.01085$] these differences have increased dramatically. The peak intensity at the interface is now 2.9. This gives a nonlinear index charge of 0.031, so that at that point the index of the nonlinear medium is higher than that of the linear medium. The beam is still totally reflected, but the output beam is now quite distorted, with two peaks.

For a further slight increase in the nonlinearity [Fig. 5(c), $n_2 = 0.011$] the same differences continue, and a new feature appears. At $z = +100$ the intensity distribution has a maximum within the nonlinear medium. This is a form of self-focused channel, but it is obviously not traveling in a straight line because by $z = +150$ it has passed back into the linear medium. Thus the beam is still totally reflected but is even more distorted. To continue our description in terms of an enhanced Goos-Hänchen shift, about half of the input power appears to have been reflected in a manner similar to the behavior of a linear interface, while the other half has undergone a very large Goos-Hänchen shift.

For a still higher nonlinearity [Fig. 5(d), $n_2 = 0.012$] the behavior starts out very similar, except that the channel in the nonlinear medium forms earlier. However, it does not curve back into the linear medium, so we now have a transmitted beam. The reflected field consists of two components. One component is similar to the reflected beam from a linear interface, except that it is somewhat distorted and broader. The other component is at a shallower angle and appears to be associated with the formation of the transmitted beam.

While the nonlinearity for Fig. 5(d) is only slightly above the threshold value for the appearance of the transmitted beam, the angle of the transmitted beam ($\psi_1 \sim 3°$) is already more than half of the incident beam angle. This suggests that small changes in the intensity of an input beam can result in comparatively large changes in the transmitted beam angle.

In the following sections we present more detailed results concerning the various features just described. The formation of a transmitted beam was not observed in one of the earlier studies of this type, so in Sec. IV.B we shall analyze that difference. We then investigate the threshold behavior in more detail, including the details of the nonlinear Goos-Hänchen shift. The final two sections give our results on the variation of the power reflectivity and the angle of the transmitted beam as functions of intensity (nonlinearity).

B. Noncoupling to Surface Wave

The beam and interface parameters and the intensity × nonlinearity product for the calculation illustrated in Fig. 5(d) are the same as for the results presented in Fig. 3 of Ref. 5, but those results show a relatively undistorted reflected beam and a surface wave with no transmitted beam. There are three differences in the way the two calculations were done. The earlier calculation[5] (1) used an Adams-Moulton integration procedure with a fixed step size in the z direction; (2) did not include a correction for the discontinuity in $\partial^2\phi/\partial x^2$ at the interface; and (3) used a mesh size of $\Delta x = 0.6$ rather than the $\Delta x = 0.15$ used in the present calculations.

In Fig. 6 we show the intensity distribution on the plane $z = +200$ calculated using the ODES integrating routine with various mesh sizes and with and without the discontinuity correction. {For the calculation without the discontinuity correction the mesh was defined such that the interface was midway between two mesh points, and the three-point formula [Eq. (11)] was used to evaluate the second derivative at those two points.} Note that for $\Delta x = 0.6$ the discontinuity correction makes a significant difference. The results without the correction [Fig. 6(d)] show a surface wave and are in excellent agreement with Fig. 3 of Ref. 5.

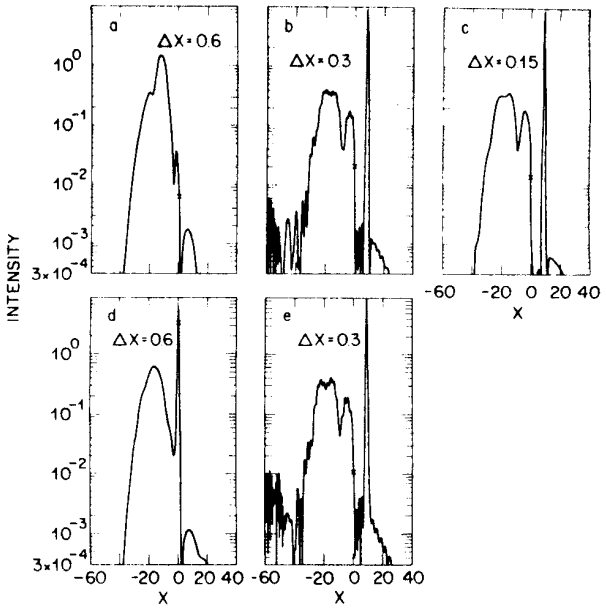

Fig. 6. Intensity distributions on the plane $z = +200$ for $n_2 = 0.012$, for various mesh spacings (Δx) and boundary conditions. For curves (a)–(c) the calculations included a correction for the discontinuity of $\partial^2\phi/\partial x^2$ at the interface as described in the Appendix. For curves (d) and (e) no such correction was made.

This agreement suggests that the differences with the present results are not because of the particular integrating routine used. For $\Delta x = 0.3$ the results show a transmitted beam, and the discontinuity correction does not seem to have a significant effect. However, the intensity distributions show a lot of noise, indicating that the integration process is becoming unstable. By decreasing Δx to 0.15 we obtain smooth distributions without any noise. Note that, except for the noise, both results for $\Delta x = 0.3$ are in good agreement with the result for $\Delta x = 0.15$.

From the above it is clear that we are operating in a region in which the results are quite sensitive to the mesh size used for the calculations. To further quantify this effect we have estimated the error in the evaluation of the $\partial^2\phi/\partial x^2$ term in the differential equation. On the basis of the plane wave[1] and surface wave theories[9,10] we expect that in general the field in the nonlinear medium will tend to be of the form $\mathrm{sech}(k_x x + x_0)$, with $k_x \sim (2\pi/\lambda)\sqrt{2n_0\Delta}$ [note Eqs. (5)–(7)]. Over most of its range the sech function can be approximated by a single exponential function, and thus we can estimate that the error in calculating $\partial^2\phi/\partial x^2$ is of the order of that of calculating the second derivative of $\exp(k_x x)$. For the three-point formula [Eq. (11)] the lowest-order term in the relative error is $(k_x\Delta x)^2/12$, while for the five-point formula [Eq. (12)] it is $-(k_x\Delta x)^4/90$. In Table I we present numerical values for various values of Δx.

From the data in Table I it is clear that for the parameters of the present calculation the three-point formula is a very poor approximation for $\Delta x = 0.6$ (~7% error per step). While the three-point formula is only used for the point on the interface and/or for the two adjacent points, the interface region is the most critical region in the problem. Thus, it is not too surprising that a mesh spacing of $\Delta x = 0.6$ gives incorrect results. At this mesh spacing the discontinuity correction also has a significant effect on the results.

As we decrease the mesh spacing we not only reduce the relative error in evaluating the derivative, we also decrease the absolute size of the region over which we use the three-point formula. The discontinuity correction is proportional to Δx [note Eq. (A3)], so it also decreases and affects a smaller region.

On the basis of the above results we conclude that the previously reported coupling between the input Gaussian beam and a surface wave[5] was an artifact of using too coarse a mesh in the calculations and of neglecting the discontinuity in the second derivative of the field at the interface. We now believe that the correct solution for this case has a transmitted beam in the form of a self-focused channel. This is the same type of solution as was found in the one other numerical study of this type,[4] although for rather different interface and beam parameters. This result is also consistent with a recent theoretical analysis based on soliton theory, which predicted that there cannot be any coupling between an incident bounded beam and a surface wave.[6]

It is interesting to note that for $\Delta x = 0.6$ the five-point formula is almost as accurate as the three-point formula is for $\Delta x = 0.15$. This suggests that if one derived higher-order approximations for the discontinuity correction, so that one could use a five-point formula for the point on the interface and for the points on either side of the interface, it might be possible to obtain accurate stable results with $\Delta x = 0.3$, thus reducing the required processor time by as much as a factor of 7.

C. Threshold Behavior and Nonlinear Goos-Hänchen Shifts

For intensities close to the threshold intensity for the appearance of a transmitted beam, the pattern of power flow in the nonlinear medium is quite complicated and a very sensitive function of the intensity (or nonlinearity). In studies of linear interfaces the power-flow patterns are typically shown by plots of intensity contours or sets of vectors indicating the intensity and direction of the power flow at various points. (See, for example, Figs. 4 and 6 of Ref. 11). While these tech-

Table I. Relative Errors in Estimating the Second Derivative of the Function $\exp(k_x x)$ Using the Three-Point Formula [Eq. (11)] and the Five-Point Formula [Eq. (12)]; the Constant k_x was Assumed to be $(2\pi/\lambda)\sqrt{2n_0\Delta}$, with $\lambda = 1$, $n_0 = 1.5$, and $\Delta = 0.02$.

Δx	$k_x\Delta x$	% error	
		3-point formula	5-point formula
0.6	0.92	7.1	0.81
0.3	0.46	1.8	0.05
0.15	0.23	0.44	0.003

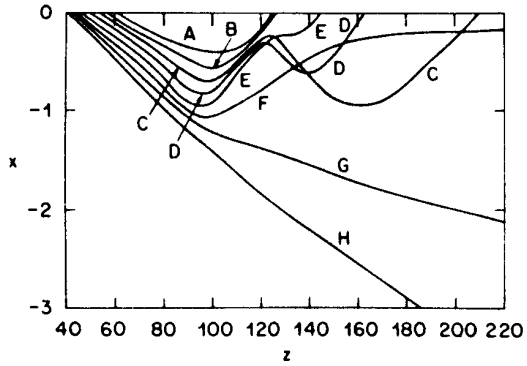

Fig. 7. Plots of the path of the peak of the self-focused channel in the nonlinear medium for various normalized intensities: $A\ n_2 = 0.01095$; $B\ n_2 = 0.01100$; $C\ n_2 = 0.01105$; $D\ n_2 = 0.01110$; $E\ n_2 = 0.01115$; $F\ n_2 = 0.01120$; $G\ n_2 = 0.01125$; $H\ n_2 = 0.01130$.

niques can be applied to the present problem, they tend to provide an overwhelming amount of detail. To present the essential features in a simpler and more compact format we have chosen just to present data on the path of the intensity maximum in the nonlinear medium. These results are shown in Fig. 7. (Note that the x and z scales differ by a factor of 40.) Despite its simplicity, Fig. 7 still contains a rich variety of features.

The curves for the lowest nonlinearities (curves A and B, with $n_2 = 0.01095$ and 0.01100, respectively) show a behavior that appears superficially similar to the Goos-Hänchen shift at a linear interface, but closer examination shows some important differences. In the linear case the power flow is more or less symmetric about the midpoint between the intersections of the incident and reflected beam axes with the interface, and the greatest penetration into the lower-index medium occurs at this point, which for our beam parameters is at $z = +12$. In the nonlinear case the maximum penetration occurs at $z \sim +100$, substantially further along the interface.

If we compare the intensity distributions for the linear interface (Fig. 3) and for the nonlinear interface with $n_2 = 0.011$ [Fig. 5(c)], we see that up to the point where the channel forms in the nonlinear medium (just beyond $z = 50$) the shapes of the distributions are very similar, but in the nonlinear case the intensity peaks are successively closer to the interface and the fields at the interface are correspondingly higher. We believe that these phenomena can be described in simple physical terms as follows. As the field propagates along the interface the evanescent field acts through the nonlinearity to reduce the index difference at the interface. This changes the phase of the reflected field such that the intensity peak moves closer to the interface and increases the intensity in the nonlinear medium. Thus, the field in the nonlinear medium increases as it propagates along the interface. The region of increased index along the interface also acts as a sort of waveguide, guiding the power along the interface, and thus extending the effect farther. If the intensity at the interface becomes sufficiently large, the intensity peak moves over to the interface and then forms a self-focused channel in the nonlinear medium. One might expect such a channel to continue to propagate in the nonlinear medium, but evidently its field distribution is sufficiently asymmetric that it undergoes a selfbending, returns to the interface, and is transmitted back into the linear medium. (Actually, a little over 1% of the power does remain in the nonlinear medium.)

The curves for the next two nonlinearities (curves C and D of Fig. 7, with $n_2 = 0.01105$ and 0.01110, respectively) display a most curious behavior. The self-focused channel curves toward the linear medium, but instead of passing through the interface it curves back into the nonlinear medium and then finally returns to the linear medium somewhat further along the interface. We do not have any explanation of this behavior, except to suggest that perhaps, where the channel first approaches the interface, the input field is sufficiently strong that additional power and asymmetry is coupled into the channel, causing it to take another bounce into the nonlinear medium. One problem with this suggestion is that for the next higher nonlinearity (curve E, with $n_2 = 0.0115$) the channel exhibits relatively little of this double bounce behavior. We note that in this case the channel penetrates farther into the nonlinear medium, but it approaches the interface in about the same region and at about the same angle as curves A–D. On balance we feel we must consider the behavior shown by curves C–E as unexplained.

The behavior represented by curve F ($n_2 = 0.01120$) is more consistent with the trend established in curves A and B, in that the channel penetrates deeper into the nonlinear medium and turns toward to the interface farther along the interface. However, the channel then appears to curve around and couple into a surface wave, seemingly contradicting the conclusions of Sec. IV.B and Ref. 6 to the effect that an input Gaussian beam cannot couple to a surface wave. However, from a more detailed examination of the behavior for $z > 200$ it is not certain that the output is a true surface wave, because the field appears to be undergoing slow oscillations and radiating its power into the linear medium. In addition, the theoretical analysis of Ref. 6 does not preclude the

possibility of coupling to a surface wave at a singular point. For the present we choose to regard the results shown in curve F as a singular result, but we invite alternative interpretations.

The final two curves in Fig. 7 (curves G and H, with $n_2 = 0.01125$ and 0.01130, respectively) exhibit simpler behavior in that once the self-focused channel is formed it continues to propagate in the nonlinear medium as a transmitted beam. Close to the interface the path is somewhat curved, but once the beam is well away from the interface it travels in a straight line. Note that a very small change in the nonlinearity makes a substantial change in the propagation direction. Note also that the fact that the transmitted light forms a self-focused channel right at the interface lends support to the hypothesis that the plane-wave theory's assumption

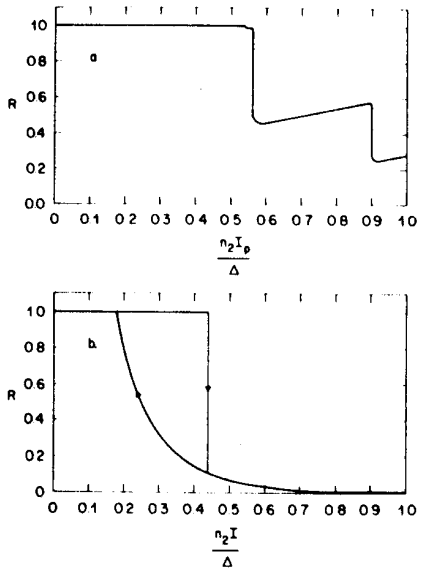

Fig. 8. Reflectivity of a nonlinear interface as a function of normalized input intensity: (a) results from the present calculations for a Gaussian beam; and (b) predictions of the plane wave theory.

of a transmitted plane wave is not valid even very close to the interface. Because we are only analyzing a 2-D configuration, the self-focused channel is stable and does not have a critical power, unlike the situation in 3-D self-focusing.[14]

D. Reflectivity vs Intensity—Bistability?

In Sec. IV.C we considered in great detail some of the microscopic properties of the interface. In this section and in Sec. IV.E we consider two macroscopic properties: power reflectivity and the propagation direction of the transmitted beam.

In Fig. 8(a) we have plotted the power reflectivity of the interface as a function of the normalized peak input intensity. The curve displays the expected sharp drop in reflectivity at the threshold intensity, but it is interesting to note that for higher intensities the reflectivity increases. This provides some limiting action such that a 50% increase in input intensity gives only a 13% increase in transmitted power.

For intensities just below the threshold the reflectivity is slightly less than unity, an effect that appears to be associated with the formation of a self-focused channel in the nonlinear medium. The transmitted power is in the form of a beam of sufficiently low intensity that it is not visible in linear plots such as Figs. 5(b) and 5(c).

A notable feature of Fig. 8(a) is that there is a second threshold at a normalized intensity of 0.9. This threshold corresponds to the formation of a second transmitted channel in the nonlinear medium as shown in Fig. 9. We have not investigated the region of the second threshold as thoroughly as we have the first threshold; however, there do not appear to be any new

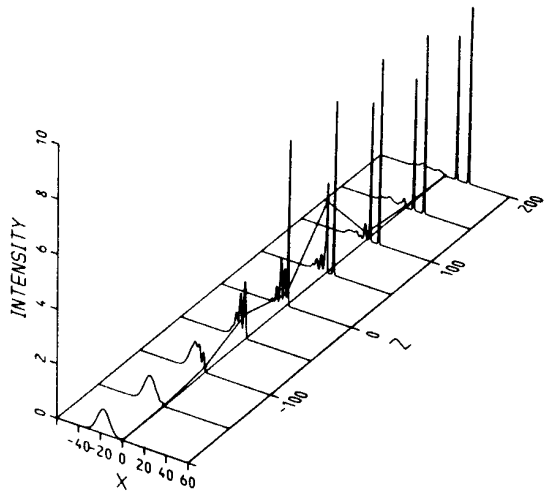

Fig. 9. Perspective plot of the intensity distributions for a nonlinear interface with $n_2 = 0.020$.

phenomena associated with the formation of the second channel. As the intensity is increased above the first threshold, the peak field at the interface, in the region beyond the point of breakthrough of the first channel, gradually increases until it is sufficient to form another channel. The formation of a second channel was also observed in the work of Rozanov.[4] We expect that calculations for still higher intensities would show a regular progression of the formation of additional transmitted channels.

For comparison with our reflectivity results, in Fig. 8(b) we plotted the reflectivity vs normalized intensity predicted by the plane wave theory[1] for a plane wave incident at the same angle as our Gaussian beam. The Gaussian beam threshold is at a normalized intensity almost 50% higher than that of the plane wave theory, but this is not unexpected, because the Gaussian beam results are normalized by the peak intensity of the

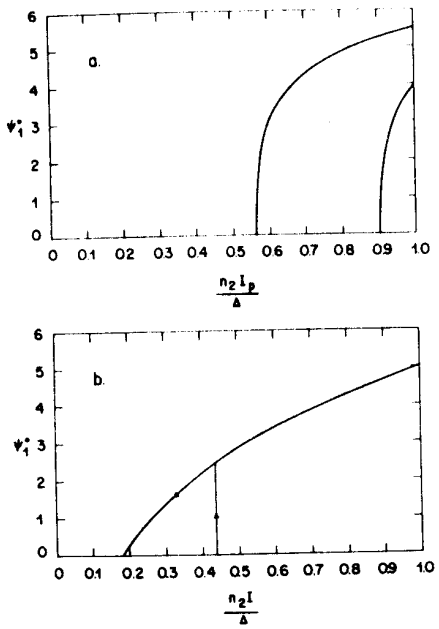

Fig. 10. Angle of the transmitted beam(s) as a function of normalized input intensity: (a) results from the present calculations for a Gaussian beam; and (b) predictions of the plane wave theory.

beam, and that intensity only exists at a single point on the interface. A possibly more significant difference is that above the first threshold the Gaussian beam reflectivity only drops to ~46%, whereas the plane wave theory predicts a drop to 10%.

The largest difference between the Gaussian beam results and the plane wave theory is that the plane wave theory predicts a bistable reflectivity, and this does not appear in the Gaussian beam results. With our present numerical simulations, it is difficult to establish (or disprove) bistability, because we are only solving a time-independent problem. Marcuse attempted to bias his integrating routine toward higher or lower intensities and observed some small differences,[5] but it now seems most likely that those differences were just a result of the insufficient number of points used for those calculations. Rozanov claims to have found bistability in some of his calculations,[4] but he did not present any of those results or give any details and has not published any further results on this question.

Our current hypothesis is that a nonlinear interface cannot exhibit bistable reflectivity for an incident Gaussian beam. This hypothesis is based on the following considerations. We consider an interface with an incident beam just above the threshold intensity and ask what will happen if the intensity of that beam is suddenly reduced to a value just below the threshold. Assuming that the intensity step is perpendicular to the axis of the input beam, the step will first affect the interface where the lower edge of the beam meets the interface (at $z \sim -200$ for our beam parameters). As the intensity step sweeps along the interface we expect the fields at the interface to rearrange themselves to just the configuration we would calculate for the lower intensity. The key point here is that all the fields propagate in the direction of increasing z, so the fields on a given constant-z plane are independent of the fields for larger z. There does not appear to be any memory mechanism to store the information on the previous field configuration, and thus it does not seem possible for the reflectivity to be bistable.

The above analysis would be invalid if a significant portion of the input field was reflected back along the interface in the direction of decreasing z. The $\partial^2\phi/\partial z^2$ term in Eq. (10), which was neglected in the present calculations, could conceivably give rise to fields propagating in that direction. Rozanov has suggested that he has found such results,[4] but we find it difficult to believe that such fields could be large enough to maintain bistability over any significant range of input intensities.

The only experimental results to date[7,8] are consistent with a bistable reflectivity, and we cannot reconcile them with the results of the current calculations. However, the experiments used only a single pulse length (~1 nsec) and thus cannot distinguish between true bistability and a transient in the material response (e.g., a transient optical damage effect).

E. Transmitted Beam Angle vs Intensity

In Fig. 10(a) we have plotted the propagation direction of the transmitted self-focused channel(s) as a function of normalized input intensity. The notable feature of these results is the very steep (but finite) slope of the curves just above the threshold intensities. These steep-slope regions may be of practical importance for producing a very rapid angular scanning of a beam.

For comparison, Fig. 10(b) gives the plane wave theory[1] results for a wave at the same angle as our Gaussian beam. The plane wave theory predicts that when the intensity is increased such that there is a transition from TIR to partial transmission, the transmitted beam will appear at a finite angle, but once the interface is in a transmitting state, the angle is a smooth function of intensity with a much smaller slope than that predicted by the Gaussian beam calculations.

V. Concluding Remarks

In this paper we have presented the results of a detailed numerical simulation of the behavior of a nonlinear interface for an incident 2-D Gaussian beam. We have found several new features in these results, and we believe that we have explained the differences between prior studies of this type. While the details of the nonlinear Goos-Hänchen shift are likely to be difficult to observe experimentally, the intensity-dependent angular scanning of the transmitted beam may have practical applications. We have only been able to investigate a single set of beam and interface parameters, but we expect that for other parameter values the same basic phenomena will occur.

The work of A. E. Kaplan was supported in part by the U.S. Air Force Office of Scientific Research. The Francis Bitter National Magnet Laboratory is supported by the National Science Foundation.

Appendix. Boundary Conditions

A. Boundary Conditions at the Interface

The propagation equation for ϕ is

$$2i\beta\partial\phi/\partial z = \phi'' + (n^2k^2 - \beta^2)\phi, \tag{A1}$$

where $\beta = n_0k\cos\psi$, and the primes indicate differentiation with respect to x. At the boundary $x = 0$, ϕ and ϕ' are continuous. If we add up Eq. (A1) taken at $x = 0 \pm \epsilon$, where ϵ is vanishingly small, we get

$$2i\beta\partial\phi/\partial z = \overline{\phi''} + (\overline{n^2}k^2 - \beta^2)\phi, \tag{A2}$$

where the superbar indicates the average of the covered quantity taken on the two sides of the boundary. No average is needed for ϕ and $\partial\phi/\phi z$ since they are continuous. To evaluate the right-hand side of Eq. (A2) we need an approximation for $\overline{\phi''}$. To obtain this we appeal to the relation

$$(\Delta x)^{-2}(\phi_1 + \phi_{-1} - 2\phi_0) = \overline{\phi''} + (\Delta x/6)\delta\phi''' + O[(\Delta x)^2], \tag{A3}$$

where $\delta\phi'''$ indicates the discontinuity of the third derivative across the boundary. Equation (A3) is derived by using the appropriate Taylor series for each side of the boundary to evaluate ϕ_1 and ϕ_{-1}. Now one can obtain an expression for the discontinuity of the third derivative by appeal to the propagation equation. Thus, differentiating Eq. (A1) with respect to x, and then taking the discontinuity of the resulting expression, yield

$$\delta\phi''' + k^2[(n_1^2 - n_0^2)\phi' + (n_1^2)'\phi] = 0, \tag{A4}$$

where again we have taken advantage of the continuity of ϕ and ϕ', and n_1 is the index of the nonlinear medium at the boundary. To obtain ϕ'' from Eq. (A3) to order Δx we need only the first approximation to the derivatives in Eq. (A4). Thus, using

$$\phi' \cong (\phi_1 - \phi_{-1})/2\Delta x;\ (n_1^2)' \cong n_0n_2[|\phi_1|^2 - |\phi_{-1}|^2]/\Delta x \tag{A5}$$

in Eq. (A4), and putting the result into Eq. (A3), we obtain

$$\overline{\phi''} = [\Delta x]^{-2}(\phi_1 + \phi_{-1} - 2\phi_0) + (k^2/12)[(n_1^2 - n_0^2)(\phi_1 - \phi_{-1}) + 2n_0n_2(|\phi_1|^2 - |\phi_{-1}|^2)\phi_0]. \tag{A6}$$

Finally, this expression is evaluated and used in Eq. (A2) to obtain $\partial\phi/\partial z$ at the points along the boundary.

B. Boundary Conditions at the Edge of the Problem

We have chosen the boundaries of our calculation to be sufficiently far from the interface ($x = \pm 60$) that there is never any significant intensity at the boundaries. However, we must take some care in defining the conditions at these boundaries to prevent instabilities from developing there. Our approach is to assume that the field on the boundaries can be approximated by a plane wave with the same propagation vector as for the field at the first point inside the boundary. Thus the second derivative of the field at the boundary is approximated by

$$\left.\frac{\partial^2\phi}{\partial x^2}\right|_n = \left.\frac{\partial^2\phi}{\partial x^2}\right|_{n-1} \times (\phi_n/\phi_{n-1}), \tag{A7}$$

where the index n indicates the point on the boundary, and $n - 1$ the first point inside the boundary.

References

1. A. E. Kaplan, JETP Lett. **24,** 114 (1976); Sov. Phys. JETP **45,** 896 (1977).
2. B. B. Boiko, I. Z. Dzhilavdari, and N. S. Petrov, J. Appl. Spectrosc. **23,** 1511 (1975).
3. A. A. Kolokolov and A. I. Sukov, Radiophys. Quantum Electron. **21,** 1013 (1978).
4. N. N. Rozanov, Opt. Spectrosc. (USSR) **47,** 335 (1979).
5. D. Marcuse, Appl. Opt. **19,** 3130 (1980).
6. A. E. Kaplan, *J. Opt. Soc. Am.* **71,** 1640 (1981).
7. P. W. Smith, J.-P. Hermann, W. J. Tomlinson, and P. J. Maloney, Appl. Phys. Lett. **35,** 846 (1979).
8. P. W. Smith, W. J. Tomlinson, P. J. Maloney, and J.-P. Hermann, IEEE J. Quantum Electron. **QE-17,** 340 (1981).
9. W. J. Tomlinson, Opt. Lett. **5,** 323 (1980).
10. M. Miyagi and S. Nishida, Sci. Rep. Res. Inst. Tohoku Univ. Ser. B. **25,** 53 (1973).
11. S. Kozaki and H. Sakurai, J. Opt. Soc. Am. **68,** 508 (1978).
12. A. E. Kaplan, Sov. J. Quantum Electron. **8,** 95 (1978); Radiophys. Quantum Electron. **22,** 229 (1979); IEEE J. Quantum Electron. **QE-17,** 336 (1981).
13. N. L. Schryer, "A User's Guides to DODES," Bell Laboratories Computing Science Technical Report 33 (1975); J. Phys. Chem. **81,** 2335 (1977).
14. S. A. Akhmanov, A. P. Sukhorukov, and R. V. Khokhlov, Sov. Phys. Usp. **10,** 609 (1968).